NUCL SCI TECH (2017) 28:164
DOI 10.1007/s41365-017-0314-8

Uncertainty of an automatic system for counting alpha tracks on CR-39

Dun-Huang Fan[1] · Wei-Hai Zhuo[1] · Bo Chen[1] · Wei-Yuan Zhang[1]

Received: 22 February 2017 / Revised: 10 April 2017 / Accepted: 12 April 2017 / Published online: 27 October 2017

Abstract For accurate counting of alpha tracks on the polyallyl diglycol carbonate of CR-39-type track detectors, the size distributions of both artifact tracks and alpha tracks were investigated with an automatic counting system. At the same temperature and etchant concentration, the numbers and sizes of alpha tracks changed significantly with the etching time, and the artifact track changes were smaller. At the etching time of 5 h, the sizes of alpha tracks were evidently larger than those of the artifact tracks, and the deviation of its size distribution was much smaller than those of longer etching time. Based on the size distribution of alpha tracks etched for 5 h, the overlap effect and uncertainty of overlap correction were studied by the Monte Carlo simulations for different track densities. It was found that the counting uncertainty of the system could be less than 6% in a density range of 10–160 tracks mm^{-2} after taking the overlap correction into account.

Keywords Uncertainty · Track counting · CR-39 · Etching · Overlap

1 Introduction

PADC of CR-39-type track detectors are widely used as passive solid-state nuclear detector to measure charged particles and neutrons due to their low cost, robustness, high detection efficiency, and small sensitivity to gamma- and X-rays and electromagnetic waves [1–3]. Heavy charged particles passing through the detectors leave latent tracks which are visible at modest optical magnification levels after chemical etching. Traditional manual methods to count the tracks are labor intensive and highly operator dependent. With the development of technology, several models of automatic counting systems have been developed, such as Radosys® and TASLIMAGE® [4–7]. In these systems, the tracks are supposed to be small light spots in uniform shapes (circular or elliptical) and counted by setting a set of binary threshold, size threshold and circularity threshold [8, 9]. However, the track discrimination will be affected by the track diameters due to different etching conditions (time, temperature, concentration, etc.), the artifact tracks (the scratches, bubbles, and small dots that are caused by the camera or detector), the energy of incident particles, etc. [10–13]. Therefore, uncertainties of the track counting should be further studied.

In this study, based on an automatic counting system developed in our laboratory for passive radon monitors, the size distributions of both artifact and alpha tracks were systematically investigated to optimize the etching conditions, and the overlap effect of alpha tracks was simulated for different monitoring conditions (track densities) to minimize and quantify the uncertainty of the counting system.

This work was supported by the National Natural Science Foundation of China (No. 11375048).

✉ Bo Chen
bochenfys@fudan.edu.cn

[1] Institute of Radiation Medicine, Fudan University, Shanghai 200032, China

2 Materials and methods

2.1 The CR-39 and its exposure

The CR-39 detector material was manufactured by Fukuvi Chemical Industry Co., Ltd, Japan. Samples in 1 cm × 1 cm size were cut from the material for experiments. A total of 128 sample detectors were randomly divided into two groups. Group A was used for investigating artifact tracks without any radon exposure. Group B were set in the passive integrated radon monitor (PIRM) we developed [14] to study the alpha tracks after exposed to 2.02 kBq m^{-3} of ^{222}Rn in a chamber for 168 h (about 340 kBq m^{-3} h of integrated radon exposure).

2.2 Chemical etching

All of the detectors were chemically etched in 6.25 N water solution of NaOH at 90 ± 0.1 °C. In order to investigate the artifact and alpha tracks in different etching periods, the etching was performed in eight stages, with 1 h for each stage. The etched samples were taken out and cleaned for track analysis.

2.3 Track analysis

Figure 1 shows the automatic track counting system we developed. It is built on an optical microscope with a ×4 objective lens and a CCD camera. A computer controlled three-dimensional mobile object stage is implemented for autofocus and the detector movements. The software in Visual C++ development environment (Fig. 1b) is responsible for the motion control, image processing, autofocusing and track counting. In routine application, the alpha tracks can be identified automatically from the artifact tracks based on the settings of binary threshold, size threshold and circularity threshold for the images. In this study, in order to obtain more information on the size and size distribution of artifact and alpha tracks, the settings of size threshold and circularity threshold were banned.

2.4 Overlap correction and its uncertainty

A Monte Carlo code was developed based on MATLAB® to investigate track overlap for different track densities. Figure 2 shows an example of the simulation regions and overlapped tracks. In the simulation, the code randomly placed tracks in the 1 mm × 1 mm simulation region and counted the tracks. To avoid the boundary effects, the simulation region was surrounded by a buffer region. As shown in Fig. 1b, most of the track images in the radon system are quasi-circular or circular; for the sake

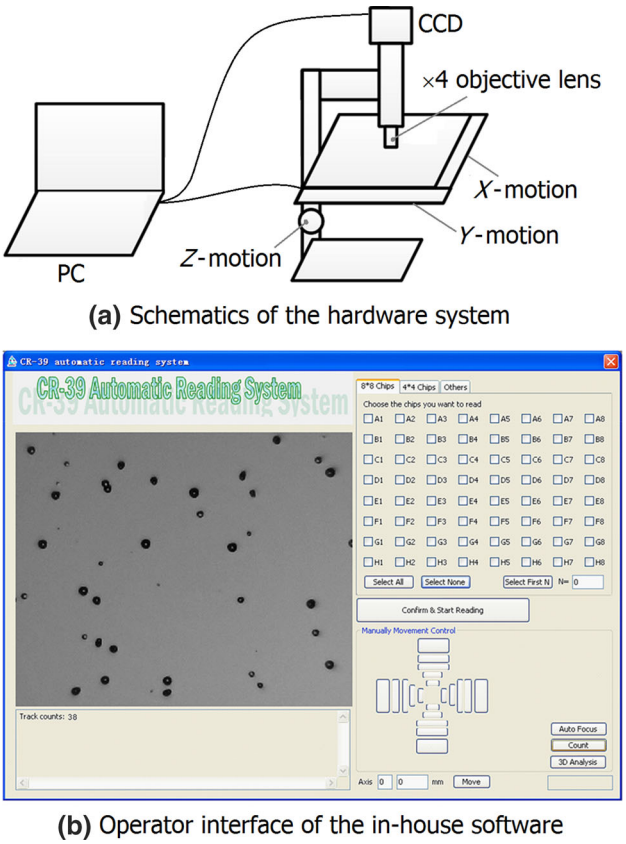

Fig. 1 Automatic track counting system

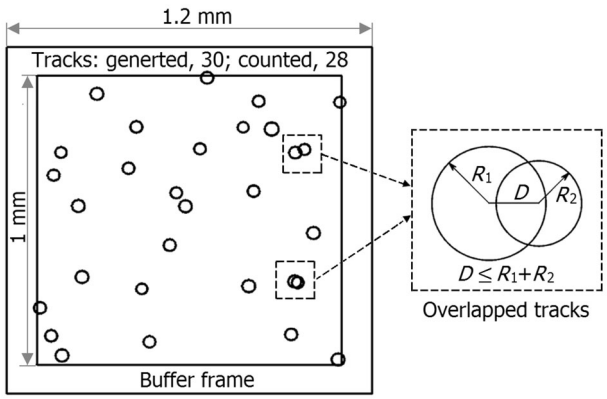

Fig. 2 Simulation region and overlapped tracks

of simplicity, circular tracks were assumed in simulation. Track diameters were chosen from measured size distributions. When the center-to-center distance of two tracks (D) was less than the sum of their radii (R_1 and R_2), i.e., $D \leq R_1 + R_2$, the two tracks were regarded as overlapped tracks and counted as one track [15].

For a specific track density of m (tracks/mm^2) generated by the code, the simulations were repeated for 20,000 times. The relative standard uncertainty for counting due to overlap effect can be estimated by [16]:

$$U_{\mathrm{OL}} = \frac{\sqrt{\sum_i^N (n_i - n_{\mathrm{mean}})^2}}{\sqrt{N-1} \times n_{\mathrm{mean}}} \quad (1)$$

where n_i is the track density counted in each simulation (tracks/mm^2); N is the repeat times of the simulations; n_{mean} is the arithmetic mean of n_i. The overlap correction factor K is defined as [17]:

$$K = m/n_{\mathrm{mean}}. \quad (2)$$

2.5 Verification of overlap correction

In order to verify the simulation results, five groups of PIRM monitors, ten pieces each, were exposed to 10 kBq m^{-3} of radon concentration in the standard radon chamber at Shanghai Institute of Measurements Technology (SIMT). The five groups were exposed to integrated radon exposures of 500–2500 kBq m^{-3} h. The exposed CR-39 detectors were etched in a 6.25 N water solution of NaOH at 90 ± 0.1 °C for the optimized etching period and counted by the auto-counting system.

3 Results and discussion

3.1 Size distribution of artifact tracks

Figure 3 shows the size distributions of artifact tracks on the CR-39 detectors without any radon exposure after etching 1–8 h. The background tracks from radon and its progeny were distinguished from artifact tracks manually. Although the number and size distribution of artifact tracks increase slightly with the etching time, most of the artifact tracks are less than 12 μm in diameter.

3.2 Size distribution of alpha tracks

Figure 4 illustrates the track images of the radon-exposed CR-39 detectors within an area of 0.5 mm × 0.5 mm after etching for 1–8 h. Some inclined tracks occur for the samples of $T \leq 5$ h, while most of the tracks become quasi-circular or circular for the samples of $T > 5$ h. This indicates that the tracks might be over-etched at $T > 5$ h [10]. Meanwhile most of the tracks enlarge with increasing etching time, hence the increase in possibility of overlapping tracks.

Figure 5 shows the size distributions of alpha tracks on the CR-39 detectors at different etching hours. They were re-plotted by subtracting size distributions of the control group from the experimental group for corresponding etching hour. Most of the tracks enlarged with etching time in different growth rates. The track sizes for 1–8 etching hours are 9.4 ± 3.3 μm (1.6–17.3 μm), 13.2 ± 4.9 μm (1.6–24.6 μm), 18.5 ± 7.2 μm (1.6–36.5 μm), 24.8 ± 9.0 μm (1.6–48.8 μm), 33.3 ± 10.9 μm (1.6–66.2 μm), 39.5 ± 13.8 μm (6.2–78.4 μm), 44.6 ± 17.3 μm (6.2–90.2 μm) and 50.1 ± 19.7 μm (6.2–96.5 μm), respectively. The standard deviation of the track sizes expanded from 3.3 μm at 1 h to 19.7 μm at 8 h. This indicates that negative effects in track counting may occur for an automatic counting system, especially in recognition of overlapped tracks.

3.3 Errors in track discrimination

Despite technique developments in automatic discrimination of tracks in the past decades [18–20], the threshold of track size was still a fundamental parameter for the automatic counting system to eliminate most of the artifact tracks. An appropriate threshold can significantly reduce uncertainty in track discrimination. In general, two types of

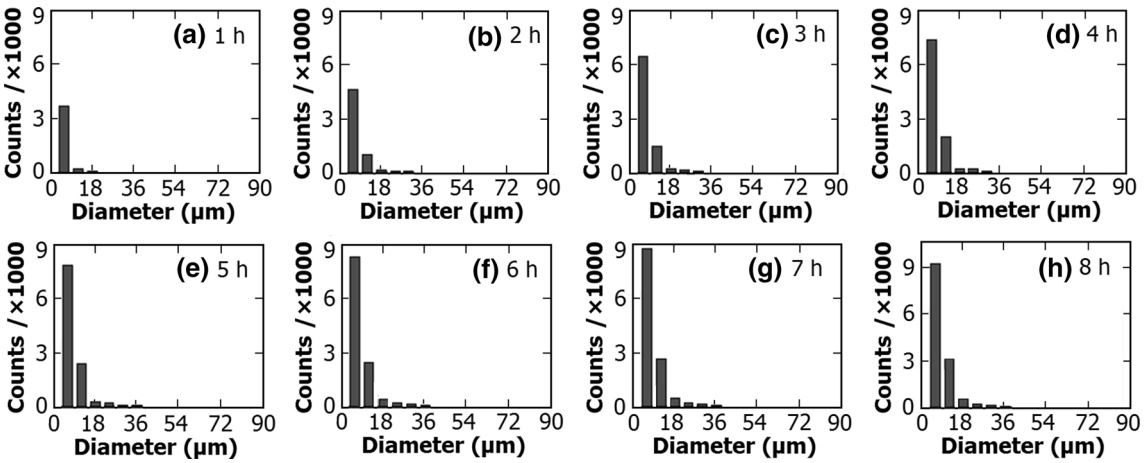

Fig. 3 Size distribution of artifact tracks for different etching hours

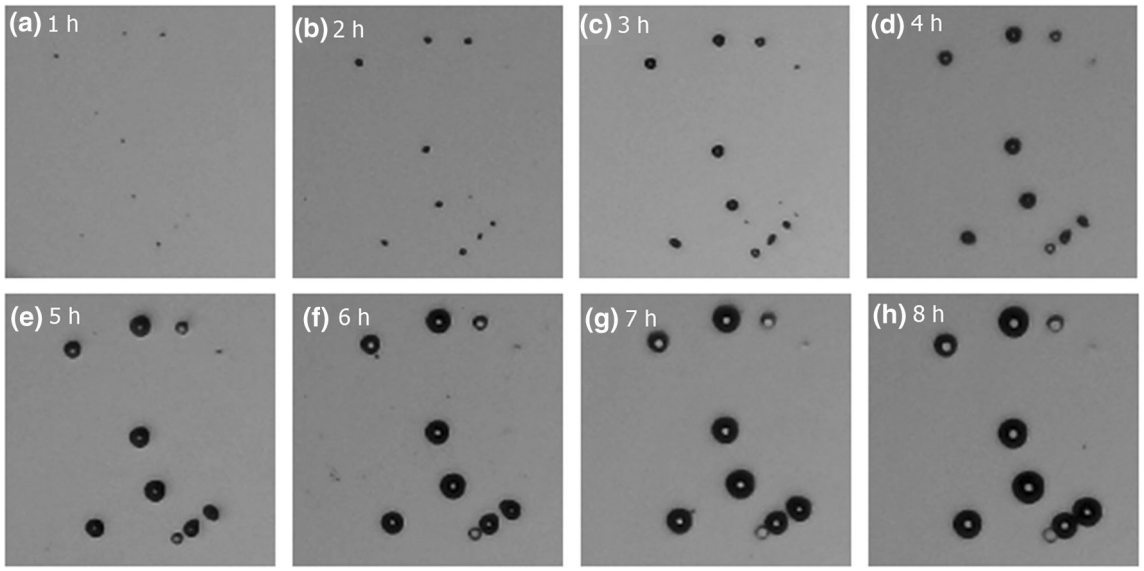

Fig. 4 Track images of the detectors etched for different hours

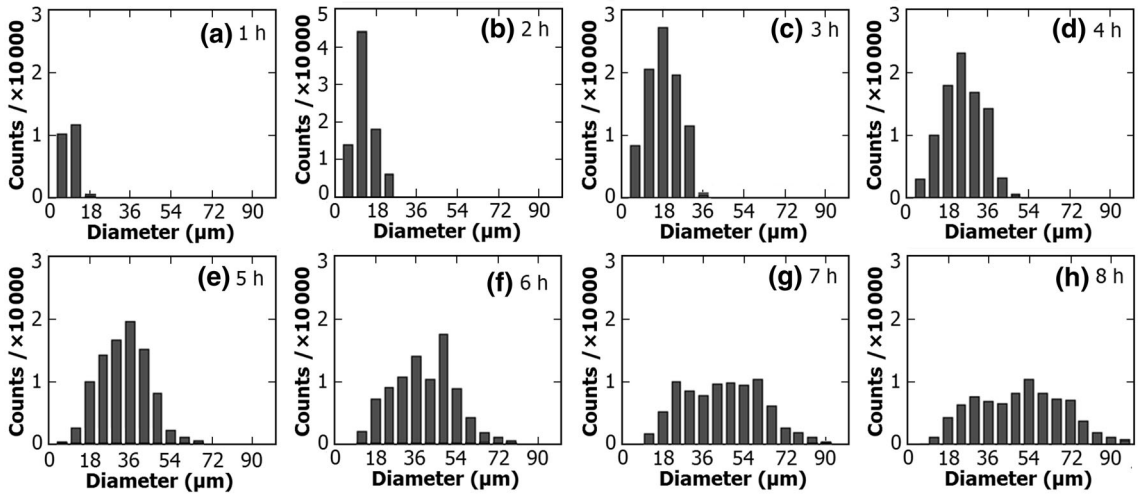

Fig. 5 Size distribution of alpha tracks for different etching time

discrimination errors are considered. Type-I is to reject small-size alpha tracks, while Type-II is to identify artifact tracks as big as alpha tracks. Having neglected the influence of geometrical parameters other than the diameter, Table 1 lists the two types of errors for different thresholds and etching time based on the experimental

Table 1 Discrimination errors (%) for different thresholds and etching time

Threshold of diameter (μm)	1 h		2 h		3 h		4 h		5 h		6 h		7 h		8 h	
	I^a	II^b	I^a	II^b	I^a	II^b	I^a	II^b	I^a	II^b	I^a	II^b	I^a	II^b	I^a	II^b
6	45.6	8.3	16.9	22.4	9.4	23.7	3.3	26.4	0.4	28.9	0.0	29.0	0.0	29.2	0.0	31.2
12	97.9	2.1	70.4	5.6	32.8	6.1	14.4	6.5	3.2	7.3	2.3	7.6	1.8	7.8	1.2	8.1
18	99.8	0.0	92.5	3.2	63.8	3.8	34.7	4.0	14.1	4.4	10.5	4.2	8.0	4.0	6.5	3.9

[a]Type-I error: the ratio of alpha tracks which are rejected

[b]Type-II error: the ratio of artifact tracks which are identified as alpha tracks

data. The results show that Type-II error deceases rapidly with the threshold, while Type-I error depends on the etching time obviously. At etching time $T = 5$–8 h, it was reasonable to set the threshold at $\Phi 12$ μm. Therefore, taking the discrimination error, deviation in track size and time cost into account, an appropriate etching time for this system is 5 h.

3.4 Overlap correction

Based on size distribution of the tracks etched for 5 h, the overlap correction curve for the simulated track densities is plotted in Fig. 6. It shows that the overlap effect may cause nearly 10% loss in track counting when the track density is 50 tracks mm^{-2}, and the counting loss will exceed 70% when the track density reaches to 200 tracks mm^{-2}. It indicates that the overlap correction is important for an accurate counting when the track density is greater than several tens.

3.5 Experimental verification results

Figure 7 shows the relationships between track density and radon exposure before and after overlap correction. The mean track density has a nonlinear response to the radon exposure, while the corrected track density has an excellent linear response to the integrated radon exposure. After overlap correction, the range of linear response for PIRM can reach to at least 2500 kBq m^{-3} h with a detection efficiency of 6.6×10^{-3} tracks cm^{-2} Bq^{-1} · m^3 h^{-1}. The results revealed that the simulation provides a reliable overlap correction.

3.6 Uncertainty of track counting

The uncertainties of alpha track counting for an automatic system mainly result from three factors, i.e., the error of track discrimination, the uncertainty due to overlap effect and the statistical fluctuation of incident particles. The error in track discrimination is usually considered as the inherent characteristics of an automatic reading system,

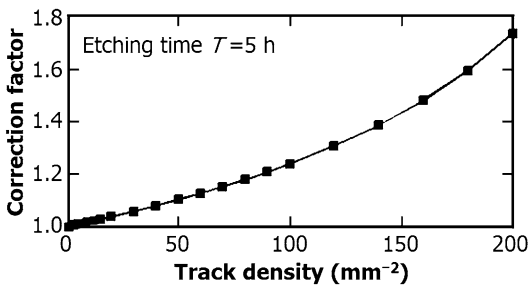

Fig. 6 Overlap correction factor for different track densities

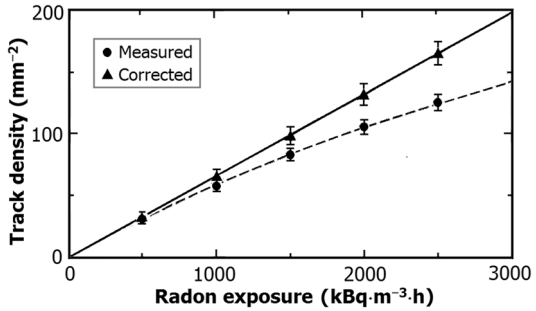

Fig. 7 Relationships between track density and radon exposure

which is determined by the mechanical and optical properties, and the discrimination strategy as well, of the system. However, the uncertainties due to overlap effect and the statistical fluctuation of incident particles depend greatly on the track density.

Figure 8 shows the two uncertainties as a function of track density. The relative standard uncertainty due to overlap effect, U_{OL}, was estimated by Eq. (1) based on Monte Carlo simulation, while the relative standard uncertainty due to statistical fluctuation was calculated by $U_{ST} = (n_{mean}\ SK)^{-1/2}$ [21], where n_{mean} is the mean track density on CR-39, in tracks mm^{-2}; K is the overlap correction factor; and S is the scanned area on each CR-39, in mm^2. The results indicate that the uncertainty due to overlap effect increases with the track density, while the statistical fluctuation shows the opposite trend. Based on the etching conditions (6.25 N of NaOH, 90 ± 0.1 °C, 5 h) in this study, it was estimated that the relative uncertainty of the track counting system would be less than 6%, at track density of 10–160 tracks mm^{-2}.

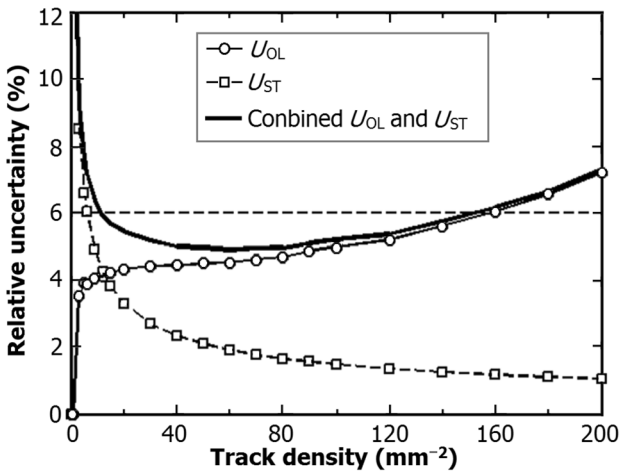

Fig. 8 Relative uncertainty for different track densities

4 Conclusion

In this study, to minimize and quantify the uncertainty of an automatic counting system, the optimal etching time and the discrimination parameters were determined through experimentally investigating the morphological characteristics of tracks on the CR-39, and the overlap correction and its uncertainty was systematically discussed. The result indicates that the overlap correction is essential for an accurate counting. By taking the overlap correction into account, the uncertainty of an automatic counting system could be controlled to be less than 6% for alpha tracks in its general application. It is expected that the results of this study would benefit the quality control for the automatic counting system.

References

1. M. Kanasaki, S. Jinno, H. Sakaki et al., The precise energy spectra measurement of laser-accelerated MeV/n-class high-Z ions and protons using CR-39 detectors. Plasma Phys. Contr. F. **58**, 034013 (2016). doi:10.1088/0741-3335/58/3/034013
2. D. Fan, W. Zhuo, Y. Zhang, Occupational exposure to radon in different kinds of non-uranium mines. Radiat. Prot. Dosim. **170**, 311–314 (2016). doi:10.1093/rpd/ncw026
3. Y. Li, X. Xia, Z. Cao et al., An experimental study on optimal chemical etching condition for CR-39 used in neutron detection. Nucl. Tech. **39**, 55–60 (2016). doi:10.11889/j.0253-3219.2016.hjs.39.060402. **(in Chinese)**
4. E. Hulber, Overview of PADC nuclear track readers. Recent trends and solutions. Radiat. Meas. **44**, 821–825 (2009). doi:10.1016/j.radmeas.2009.10.097
5. D.L. Patiris, K. Plekas, K.G. Ioannides, TRIAC: a code for track measurements using image analysis tools. Nucl. Instrum. Meth. B **244**, 392–396 (2006). doi:10.1016/j.nimb.2005.10.026
6. M. Dolleiser, S.R. Hashemi-Nezhad, A fully automated optical microscope for analysis of particle tracks in solids. Nucl. Instrum. Meth. B **198**, 98–107 (2002). doi:10.1016/S0168-583X(02)01484-2
7. V.A. Ponomarenko, J. Molnar, An automatic image analysis system for the evaluation of dielectric track detectors. Radiat. Meas. **34**, 187–188 (2001). doi:10.1016/S1350-4487(01)00148-2
8. A. Segovia, M. Garduno, M. Balcazar et al., Automatic evaluation of solid state track detectors by artificial vision. Comput. Electr. Eng. **39**, 274–284 (2013). doi:10.1016/j.compeleceng.2012.11.010
9. A.G. Hoon, L. Jai-Ki, Construction of an environmental radon monitoring system using CR-39 nuclear track detectors. Nucl. Eng. Technol. **37**, 395–400 (2005). **(in Chinese)**
10. D. Nikezic, K.N. Yu, Formation and growth of tracks in nuclear track materials. Mater. Sci. Eng., R **46**, 51–123 (2004). doi:10.1016/j.mser.2004.07.003
11. G. Gillmore, D. Wertheim, S. Crust, Effects of etching time on alpha tracks in solid state nuclear track detectors. Sci. Total Environ. **575**, 905–909 (2017). doi:10.1016/j.scitotenv.2016.09.147
12. M.F. Zaki, Y.H. El-Shaer, Particularization of alpha contamination using CR-39 track detectors. Pramana-J. Phys. **69**, 567–574 (2007). doi:10.1007/s12043-007-0156-8
13. W. Zhuo, B. Chen, D. Li et al., Experimental study on CR-39 response to alpha particles with different incident angles and energy. At. Energy Sci. Technol. **42**, 322–325 (2008). **(in Chinese)**
14. C. Zhao, W. Zhuo, D. Fan et al., Effects of atmospheric parameters on radon measurements using alpha-track detectors. Rev. Sci. Instrum. **85**, 022101 (2014). doi:10.1063/1.4865155
15. A.B. Zylstra, J.A. Frenje, F.H. Seguin et al., A new model to account for track overlap in CR-39 data. Nucl. Instrum. Meth. A **681**, 84–90 (2012). doi:10.1016/j.nima.2012.04.021
16. O. Hanley, J.L. Gutierrez-Villanueva, L. Currivan et al., Assessment of the uncertainties in the Radiological Protection Institute of Ireland (RPII) radon measurements service. J. Environ. Radioact. **99**, 1578–1582 (2008). doi:10.1016/j.jenvrad.2007.12.018
17. I. López-Coto, J.P. Bolívar, A theoretical model for the overlapping effect in solid state nuclear track detectors. Nucl. Instrum. Meth. A **652**, 550–553 (2011). doi:10.1016/j.nima.2010.12.223
18. Y. Luo, Y. Zhou, J. Xiao et al., Measurement of solid state nuclear track parameter. Nucl. Tech. **22**, 590–593 (1999). **(in Chinese)**
19. A. Boukhair, A. Haessler, J.C. Adloff et al., New code for digital imaging system for track measurements. Nucl. Instrum. Meth. B **160**, 550–555 (2000). doi:10.1016/S0168-583X(99)00628-X
20. S. Paul, S.P. Tripathy, P.K. Sarkar, Analysis of 3-dimentional track parameters from 2-dimensional images of etched tracks in solid polymeric track detectors. Nucl. Instrum. Meth. A **690**, 58–67 (2012). doi:10.1016/j.nima.2012.06.054
21. T. Iida, Q.J. Guo, Y. Ikebe, Some problems on the measurement of ^{222}Rn concentrations by passive cup method. Health Phys. **69**, 508–512 (1995). doi:10.1097/00004032-199510000-00009